Journal of Analytical and Applied Pyrolysis 156 (2021) 105100

Contents lists available at ScienceDirect

Journal of Analytical and Applied Pyrolysis

journal homepage: www.elsevier.com/locate/jaap

Synergistic effects of biomass building blocks on pyrolysis gas and bio-oil formation

Andrew H. Hubble, Jillian L. Goldfarb *

Department of Biological and Environmental Engineering, Cornell University, Ithaca, NY, 14853, USA

ARTICLE INFO

Keywords:
Pyrolysis
Polysaccharide
Biomass
Mixture
Synergy
Bio-oil

ABSTRACT

Before biobased fuels can replace fossil fuels, several key issues must be addressed. Bio-oils derived through pyrolysis of lignocellulosic material have high acidity and viscosity, and poor energy density and stability. To address these issues, this paper examines the individual and combined behavior of lignocellulosic feedstock components to shed light on the potential to generate preferential biofuel properties through biomass mixing. Dry lignocellulosic biomass is mostly composed of cell wall polysaccharides (cellulose, hemicellulose, lignin), which vary widely in type and concentration across biomasses. This heterogeneity leads to increased unpredictability in biobased fuel formation during pyrolysis. Using derivative thermogravimetric (DTG) analysis, gas chromatography-mass spectroscopy, and residual gas analysis, this work explores the synergistic interactions of lignocellulosic biomass components during pyrolysis to manipulate bio-oil and gas product composition based on desired compound classes. Cellulose, xylose, xylan, and lignin were blended at different ratios to determine the extent of synergistic effects during pyrolysis. For each mixture, an 'expected' outcome was developed by summing the individual behavior (e.g. mass loss rate, H_2 gas evolution, etc.) of the individual components based on mass fraction present. Mixtures containing lignin and/or xylan yield peak DTG mass loss rates at lower temperatures than predicted with corresponding reductions in biochar yield suggesting synergistic interactions that promote devolatilization. By itself, lignin produces large amounts of hydrogen gas, and when mixed with other biomasses promotes dehydrogenation. Lignin increases CO_2 formation, resulting in lower oxygen concentrations in the bio-oil and biochar. While suppressing bio-oil generation, the presence of lignin – even at low concentrations – increases the number of phenol compounds produced, while decreasing the yield of furans. The synergistic interactions between different polysaccharides could be exploited depending on the desired biorefinery products – allowing for targeted selection of lignocellulosic biomass mixes to fine-tune resulting fuels.

1. Introduction

When left to naturally decompose, agricultural waste generates methane, a potent greenhouse gas [1]. This can be avoided by harvesting waste biomass before it decomposes and using it as a feedstock for generating sustainable biofuels. However, current biofuel production utilizing thermochemical pathways (such as pyrolysis, thermochemical devolatilization at elevated temperatures under an inert atmosphere) with biomass waste feedstocks is limited by numerous factors, including: process energy requirements, poor bio-oil stability and quality, as well as downstream catalyst costs, fouling, and regeneration issues with upgrading the fuel to a usable form [2–4]. These problems are surmountable; one potential avenue is manipulating the feedstock composition to reduce or remove large oxygenated tar compounds and promote the formation of small aromatic ring structures.

Lignocellulosic plant matter is primarily comprised of polysaccharides and polyphenols of three major component classes: cellulose, hemicellulose, and lignin. While the pyrolysis of each of these constituents individually is well studied [5–8], the behavior of individual components is not necessarily an accurate representation of how the biomass behaves as a whole during pyrolysis. As such, we must understand to what extent biomass building blocks interact during pyrolysis to promote or suppress product formation. This will allow for better selection of biomass feedstocks and blends to enable upstream tuning of downstream products formed.

Cellulose is composed of long chains of glucose monomers with each successive molecule rotated 180° around the axis of the polymer backbone chain. Cellulose depolymerizes and forms free radicals at pyrolysis

* Corresponding author.
E-mail address: JillianLGoldfarb@gmail.com (J.L. Goldfarb).

https://doi.org/10.1016/j.jaap.2021.105100
Received 18 September 2020; Received in revised form 16 January 2021; Accepted 9 March 2021
Available online 14 March 2021

temperatures above 100 °C. Up to 300 °C, cellulose pyrolysis results in the formation of carbonyl and carboxyl groups, CO and CO_2, and biochar, a solid carbonaceous residue [9]. From 300−450 °C, cellulose's glucose monomers begin to open and dehydrate, forming levoglucosan (a dehydrated glucose ring) and other anhydrides and oligosaccharides [10–12]. Tar compounds (e.g. levoglucosan) formed over this temperature regime result in a liquid bio-oil that is acidic, unstable, and heavily oxygenated [13,14]. Above 450 °C, smaller carbonyl compounds such as acetaldehyde, glyoxal, and acrolein form, which are more desirable than large tar compounds from the previous phase [10,15–17].

Hemicellulose is a family of complex polysaccharides associated with cell wall composition and contains branched structures which differ across plant species. Hemicellulose decomposes at lower temperatures as compared to cellulose. It is very reactive above 100 °C, and is a large driver of furan production [18–22], often considered a desirable product for the integrated biorefinery [23]. The most abundant hemicellulose, xylan [20,21], yields eight main products while undergoing thermal decomposition: water, methanol, acetic acid, formic acid, propionic acid, hydroxyacetone, acetoin, and furfural [24].

Lignin is a long-order, highly cross-linked polymer comprised of phenolic compounds, and is a major component of woody biomass. Lignin imparts structural stability – allowing plants to grow tall without collapsing under their own weight. It devolatilizes at higher temperatures than cellulose or hemicellulose. Extensive cleavage of one of the most prevalent and well-understood linkage types (β-aryl ether or β-O-4) begins around 270 °C and peaks at 350−450 °C. As the dominant linkage in many lignocellulosic biomasses, scission of β-aryl ether (and similar linkages) yields products that resemble the individual phenolic monolignols [10,25–28]. Since lignin has a highly aromatic structure, it tends to produce more aromatic compounds upon pyrolysis.

Each of these polysaccharides devolatilizes at different temperatures owing to their varying compositions, structures, and degree of polymerization, and each produces different products upon pyrolysis. Understanding how these constituents interact during pyrolysis, and to what degree they promote or inhibit devolatilization, is key to understanding what products can be expected from different feedstocks. If these components do not interact, the products would simply be a summation of their individual parts. Interaction between polysaccharides could promote favorable compound formation, or aid in the reduction of non-desirable tar or heavily oxygenated compounds.

Previous studies indicate that blends of cellulose, hemicellulose, and lignin show both additive and non-additive (synergistic) behavior [29,30]. Additive blends are those where the components devolatilize according to their individual behavior, such that their kinetics can be described as the weighted sum of the mixtures' parts, and the products evolved are similarly a weighted average. Much like an ideal gas mixture, an additive blend is one where the individual components do not "see" each other, and therefore do not interact. In non-additive (synergistic) reactions, one species assists another in devolatilizing, often at lower temperatures than individual components, or prevents the devolatilization of the other. Devolatilization can be hampered either via direct inhibition of the process, or an antagonistic effect. Xue et al. pyrolyzed cellulose and starch up to 900 °C to observe changes in mass loss regimes and activation energy [31]. Cellulose and starch have identical monomers but differ in linkage types in the polymer structure (α vs. β). Even this minor difference in linkage type among otherwise identical biomasses revealed non-additive behavior: mixtures with at least 50 % starch content promoted cellulose devolatilization at lower temperatures. This non-additive behavior is a promising indication of synergistic interaction where a component devolatilizing at lower temperatures can effectively catalyze compounds typically devolatilizing at higher temperatures.

Liu et al. blended cellulose, hemicellulose (xylan), and lignin in various quantities and pyrolyzed said mixtures up to 800 °C [32]. An analysis in changes of derivative thermogravimetric (DTG) curves yields experimental mass loss peaks which differ from the experimental additive scheme. The constituents – in the presence of one another – changed the bulk mixture behavior and either raised (cellulose and hemicellulose) or lowered (hemicellulose and lignin) the peak reaction temperature. Lowering peak reaction temperature through biomass blending could reduce the economic barriers to biomass pyrolysis at an industrial scale by reducing energy input. Such blending can also be used to tune downstream product distribution; for example, in Liu et al.'s work, hemicellulose and lignin containing mixtures showed lower furfural yield and fewer C═O containing functional groups such as ketones and aldehydes in the pyrolysis bio-oil than cellulose containing mixtures. However, Liu et al. do not report pyrolysis results for lignin individually in this work. Without a pure lignin baseline, it's difficult to quantify synergistic reactions. The near-linear decrease in functional groups could be attributed directly to the decreased quantity of hemicellulose and not any interaction [32].

In contrast, Chen and Kuo torrefied cellulose, hemicellulose, and lignin blends up to 300 °C, with little evidence of synergistic effects. The mass loss regimes observed indicated that the combined effects are solely additive, and that little or no promotion of devolatilization exists across species [33]. It is likely that the low-temperature range over which torrefaction occurs does not produce synergistic effects, as lignin is only in the initial stages of decomposition and cellulose has just begun ring-opening and levoglucosan production.

Many studies utilize DTG curves to represent total devolatilization reactivity. While DTG is informative of the degree of synergistic effects related to mass loss rates and peak temperatures (indicative of overall reaction kinetics [34]), it does not ultimately reveal the effect on the biochar, bio-oil, and gas products formed during pyrolysis, which is at the heart of feedstock decision-making. To complement DTG analysis, this paper utilizes gas chromatography–mass spectroscopy (GC–MS) to identify major bio-oil components, and residual gas analysis (RGA) via mass spectroscopy to identify the non-condensable gas formed during pyrolysis in real-time. This work explores the potential synergistic effects between cellulose, xylan (hemicellulose polymer), xylose (hemicellulose monomer), and lignin to enable an improved understanding of how biomasses behave during pyrolysis and the potential to tune the quantity and quality of pyrolysis products based on feedstock composition.

2. Materials and methods

Four individual biomass constituents: cellulose (MP Biomedicals microcrystalline cellulose powder, minimum 97 % pure, 162.14 g/mol), xylan (TCI xylan from corn core, minimum 95 % pure), xylose (Alfa Aesar D-(+)-xylose, >99 % pure, 150.13 g/mol), lignin (Sigma Aldrich low sulfonate content alkali lignin, density 1.3 g/mL) were used (as received) individually, and as mixtures in the weight ratios given in Table 1. Mixtures were fabricated by weighing the individual components to the 0.1 mg on a Shimadzu Analytical Balance directly into a clean glass vial and vortex mixing to ensure homogeneity.

Table 1
Biomass constituent mixtures.

Mixture	Cellulose (wt %)	Xylose (wt %)	Xylan (wt %)	Lignin (wt %)
1	50	—	—	50
2	50	—	50	—
3	50	50	—	—
4	—	50	—	50
5	—	50	50	—
6	—	—	50	50
7	33	—	33	33
8	33	33	—	33

2.1. Generation of pyrolysis bio-oil

Approximately 2.5 g of each sample was weighed into a porcelain combustion boat and inserted into a 2-inch diameter quartz tube furnace (MTI single heating zone GSL-1100X). A nitrogen gas generator (Parker Balston Model N2-04) supplied the inert atmosphere necessary for pyrolysis, with an Omega mass flow controller (FMA-5500) delivering 100 ml/min of N_2 (<0.1 % O_2). We purged the tube furnace and subsequent cold traps for 10 min before heating began to ensure an inert atmosphere. The furnace temperature was ramped at 10 °C/min from ambient to 110 °C and held for 30 min remove residual moisture. The temperature was then raised to 600 °C at 10 °C/min and held for 60 min, at which point the furnace was allowed to cool to 80 °C under N_2 to ensure no oxygen infiltration into the system. The biochar sample was weighed to determine the mass fraction of char recovered (solid yield).

The setup downstream of the tube furnace included a set of four glass cold traps (to collect condensable bio-oils), the capillary for the residual gas analyzer (RGA, to analyze non-condensable gases), and finally a water trap after which the residual pyrolysis gas was vented into a fume hood. Transfer lines from the furnace to the cold traps were maintained at 250 °C using heating tape, (Omega model FGH101-040 L; Staco Energy variable transformer model 3PN1010B) to prevent bio-oil condensation in the lines to the cold traps. The cold traps were suspended in vacuum flasks surrounded by a dry ice and glycol mixture. The first two cold traps in series condensed all of the bio-oil; the second two traps served as additional protection for the RGA (Extorr XT300 M with Pfeiffer HiCube 80 Eco Vacuum). The RGA analyzed the non-condensable gases in real time via a 40 μm inner diameter silica glass capillary. Mass to charge (m/z) ratios for four gases were monitored: hydrogen ($m/z = 2$), methane ($m/z = 15$), ethane ($m/z = 27$), and carbon dioxide ($m/z = 44$). Due to the overlap of spectra peaks, secondary peaks for methane ($m/z = 15$) and ethane ($m/z = 27$) are used in this analysis [35].

2.2. Bio-oil characterization via gas chromatography - mass spectroscopy

The glass cold traps used for bio-oil collection were weighed at the beginning of the experiment, after bio-oil collection, and after bio-oil extraction. The difference in weight between collection and baseline represents the bio-oil generated, and the difference between extraction and collection determines the amount of recoverable bio-oil. To extract the bio-oil, 5 ml of dichloromethane (DCM) was added to the second cold trap and used to rinse the glassware of as much bio-oil as possible. This DCM and bio-oil solution was transferred to the first cold trap, and another 5 ml DCM was used to rinse the first trap. The resulting mixture contained 10 ml DCM and a known quantity of bio-oil weight (by difference).

Before analyzing the bio-oil, the water produced during pyrolysis was removed by drying 1 ml of dissolved oil over approximately 0.1 g of anhydrous magnesium sulfate (AMS) (Fisher Scientific) in a 1.5 ml polypropylene centrifuge tube. The empty centrifuge tube weight, and weight with AMS were both recorded. The centrifuge tube was filled with the (DCM + bio-oil) solution to a total volume of approximately 1.2 mL. The total weight was recorded. The tube was shaken by hand for approximately four minutes, then centrifuged for two minutes. Any water previously in the oil, now bound to the AMS, was separated to the bottom of the centrifuge tube. Water generated during these experiments was less than 1% of the pyrolysis bio-oil, by weight. The bio-oil was pipetted out and placed into a new centrifuge tube for storage (weighed before and after). The old centrifuge tube with the remaining AMS and water was weighed immediately, and represented the mass of the tube, hydrated AMS, and residual organics. The tube was left uncapped in the fume hood for several days to evaporate any residual bio-oil and DCM, over which time it was weighed 2–3 more times until the weight stabilized to determine an approximate bio-oil water content.

The dried bio-oil was analyzed via gas chromatography–mass spectroscopy (GC–MS, Shimadzu GC–MS-QP2020 with AOC-20s Autosampler). 0.2 mL of the dehydrated bio-oil was diluted with 0.5 mL DCM prior to injection. The oven temperature was set to 40 °C, and the sample was injected at 250 °C onto a Shimadzu Crossbond 30 m long, 0.25 mm ID column, with a flow of 1 ml/min helium and a split ratio of 15:1. The oven was held at 40 °C for 5 min before ramping at 5 °C/min to 150 °C and holding for 5 min. The oven was ramped again at 1.75 °C/min to 250 °C and held for 10 min. Interface and ion source temperatures were 250 °C and 230 °C respectively. A solvent cut time of 6 min was set on the mass spectrometer, after which time it was run in scan mode from 15 to 400 m/z using electron ionization. Peaks with slopes ≥1500, and durations ≥2 s on the resulting chromatogram were isolated and analyzed. Compounds were identified by spectra through the internal NIST library and a series of marker compounds were confirmed with calibration solutions.

2.3. Thermal analysis of biomass pyrolysis

In addition to pyrolyzing samples in the tube furnace, approximately 10 mg of each biomass (pure compounds and mixtures) was analyzed on a TA Instruments Discovery series 650 thermogravimetric analyzer (TGA). The same run was used for proximate analysis and to construct pyrolysis derivative thermogravimetric (DTG) curves. In step 1 of the TGA run, samples were heated under nitrogen to 110 °C and held for 30 min to drive off moisture. In step 2, samples were pyrolyzed by heating to 900 °C at a rate of 10 °C/min and held for 60 min at 900 °C. This pyrolysis step represents the mass loss of volatile matter, and the mass at the end of this step was used to calculate the DTG curves. Following this step, samples were exposed to dry air and heated to 950 °C and held for an additional 15 min (mass loss attributed to fixed carbon; residual inorganic mass is loosely termed "ash"). During the TGA run, the mass of the sample is collected every 0.5 s, which allows for the construction of a derivative thermogravimetric (DTG) curve showing the mass loss profile of the sample, and the temperature range where the majority of the volatile matter is lost, as well as providing information for a proximate analysis. The mass loss converted at any time t, X(t), during the pyrolysis step was determined via Eq. 1:

$$X(t) = \frac{m_{dry} - m_t}{m_{dry} - m_{pyr}} \quad (1)$$

Where m_{dry} is the mass after the sample is held at 110 °C (at the start of pyrolysis), m_t is the mass at any time, t, during the pyrolysis TGA step, and m_{pyr} is the residual mass left at the end of the 60 min pyrolysis at 900 °C. DTG curves were constructed by plotting dX/dt versus temperature.

Table 2
Proximate Analysis of Individual Components and their Mixtures (± one standard deviation).

Pyrolysis Feedstock (Mixtures are equal mass)	Volatile Matter (wt % dry basis)	Fixed Carbon (wt % dry basis)
Cellulose	97.4 ± 1.3	2.6 ± 1.3
Xylan	56.8 ± 4.9	43.2 ± 4.9
Xylose	82.7 ± 1.5	17.3 ± 1.5
Lignin	82.1 ± 3.2	17.9 ± 3.2
Cellulose + Lignin	70.5 ± 2.2	29.5 ± 2.2
Cellulose + Xylan	86.7 ± 2.0	13.3 ± 2.0
Cellulose + Xylose	90.0 ± 1.9	10.0 ± 1.9
Xylose + Xylan	80.4 ± 2.1	19.6 ± 2.1
Lignin + Xylan	64.9 ± 0.2	35.1 ± 0.2
Lignin + Xylose	63.8 ± 3.5	36.2 ± 3.5
Cellulose + Xylan + Lignin	68.5 ± 0.2	31.5 ± 0.2
Cellulose + Xylose + Lignin	69.1 ± 1.8	30.9 ± 1.8

3. Results and discussion

3.1. Proximate and thermogravimetric analysis

Proximate analysis for the individual and mixed biomasses are presented in Table 2. Since all biomass components were purchased at high purity, as expected negligible ash was observed. Lignin and lignin containing mixtures presented higher fractions of fixed carbon.

Representative derivative thermogravimetric (DTG) curves for five mixtures and the individual polysaccharides are plotted in Fig. 1 (additional DTG curves available in online Supplemental Information, SI). Each of the five mixtures are compared directly to a predicted outcome (labeled as *expected*).

To develop the expected (additive or non-synergistic) behavior, individual properties were weighted by mass fraction and the weighted fractions added together. Eq. 2 below depicts the general formula

$$P_{expected} = \sum_{i=1}^{n} x_i P_i \quad (2)$$

where $P_{expected}$ is the property of interest of the mixture (e.g. amount of hydrogen formed, mass loss rate, furans produced, etc.), x_i is the mass fraction of each polysaccharide in a mixture, according to Table 1, and P_i is the property that results from pyrolysis of the individual component.

If two biomasses are co-pyrolyzed and do not interact, then the outcomes – in either gas evolution, bio-oil formation, or mass loss rates – should be an additive (non-synergistic) function of each pure component's contribution to the mixture. If the two biomasses interact by promoting or suppressing devolatilization, then the DTG curves will diverge. In Fig. 1, the combination of cellulose and lignin resulted in a depressed peak mass loss rate, and a slight shift to a higher temperature. In the cellulose-lignin case, the mass remaining after pyrolysis is close to the prediction. The cellulose and xylan mixture exhibits similar behavior to the predicted case, however with a slightly increased peak mass loss rate. The increase in the peak mass loss rate at elevated temperatures translates to a reduction in the effectiveness of pyrolysis at lower temperatures for this mixture. Cellulose is the likely driver for this, as it overpowers the xylan which tends to devolatilize at lower temperatures. The decrease in low temperature devolatilization hints at an overall reduction in mass loss, resulting in greater solid biochar yield.

Additionally, Fig. 1 shows cellulose volatilizing in a single large peak, where xylan, xylose, and lignin undergo a longer, multi-step decomposition. Of the compounds analyzed in this work, cellulose is the simplest and most uniform in its construction. Single chains of glucose monomers behave uniformly when evenly heated, depolymerizing and devolatilizing together within a small temperature window

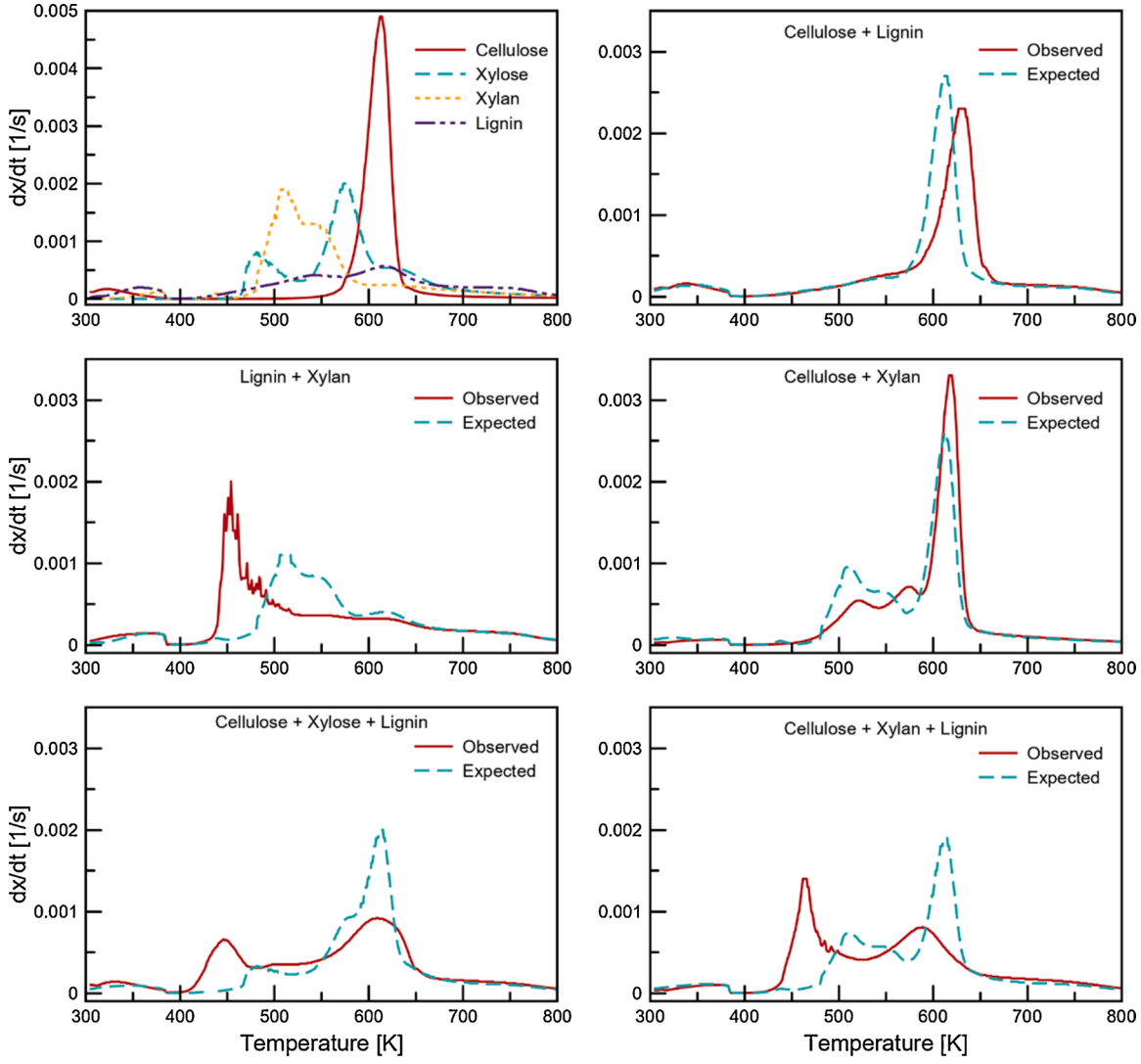

Fig. 1. Representative derivative thermogravimetric mass loss curves of polysaccharide mixtures showing observed data versus expected mixture behavior as calculated via Eq. 2.

[36,37]. In contrast, lignin is highly polymerized with a variable structure. Some components of lignin may begin to pyrolyze at relatively low temperatures, while others are only affected at high temperature. This variability gives a much longer devolatilization time, and spreads the mass loss over a wider temperature range [9,38]. Hemicelluloses, such as xylan, behave somewhere in the middle of cellulose and lignin. Hemicelluloses tend to have long single-chain backbones like cellulose, but contain branching structures like lignin. These branched structures undergo scission and are removed from the backbone (completely or in part) where they break down and behave differently [9,39]. Xylose, as a monomer, would be expected to devolatilize in a manner similar to cellulose. However, the dual-peak nature of xylose may be indicative of several mechanisms. Huang et al. proposed several reaction pathways for the breakdown of xylose. These independent peaks could be competing dominant parallel pathways, or a delay in a single pathway – where the reaction is carried partway, but requires sufficiently high temperatures for the next steps, resulting in a lag in the volatilization behavior [40].

The largest differences between expected and observed thermal behavior are seen in the lignin and xylan containing mixtures. The peak mass loss rate for the lignin and xylan mixture increases considerably at lower temperatures compared to the predicted profile. In addition, each mixture saw an 8–10 % drop in biochar yield, indicating more biomass was converted into oil and gas. The increased devolatilization indicates synergistic effects between the two compounds.

The total mass loss is governed by the area under the DTG curve, and normalized to the mass of the sample; this total area is equal to 1. A shift in the peak from right to left (or the more area at the lower end of the spectrum) equates to increased conversion at lower temperatures, improving the energy efficiency of the conversion process.

Mixtures containing xylan (or xylose) with lignin had significant reductions in the peak temperature, and saw concentrated devolatilization over narrower temperature ranges. Lignin and hemicellulose individually devolatilize over a wider thermal range than cellulose, however when lignin and hemicellulose are mixed, their devolatilization becomes concentrated at low temperatures. In contrast, cellulose containing mixtures either raised the peak temperature, or suppressed devolatilization at lower temperatures. Cellulose devolatilizes over a narrow and elevated temperature range and tends to dominate when mixed with one other biomass. However, mixtures containing all three biomass types benefitted from devolatilization at lower temperatures. When cellulose is mixed with two biomasses, its effects become suppressed.

3.2. Residual gas analysis

Non-condensable gases offer insight into the pyrolytic devolatilization pathways. Fig. 2 displays the evolution of the pyrolysis gas from all four individual biomasses and highlights the outlier: lignin. Lignin is composed of approximately 4.9 % hydrogen by weight [41], whereas cellulose, xylose, and xylan have 6.2 wt%, 6.0 wt%, and 5.3 wt% respectively. While all four raw polysaccharides contain roughly similar amounts of hydrogen, lignin produces nearly ten times the amount of hydrogen gas. The exact mechanism for this result is not well understood. However, lignin, a large and non-uniform polymer, depolymerizes and volatilizes non-uniformly. This presents a potential for greater errant functional groups, which when further reacted are a source of hydrogen gas [42,43]. The greater removal of hydrogen leads to more C—C and C—O bond preservation/formation, favoring biochar over liquid bio-oil generation. All samples produce similar quantities of carbon dioxide over the reaction time (peak temperature of 600 °C is reached at 90 min), and the peak evolution for each of the four gases occurs at approximately the same time. Carbon dioxide is driven from the samples before the bulk of hydrogen gas is released/formed, and methane is largely formed before ethane during cellulose, xylose, and xylan pyrolysis although in lower amounts.

Four gases (hydrogen, carbon dioxide, methane, and ethane) were tracked for all 8 mixtures. Gas generation increased above the expected values in 31 of 32 cases, seen in Table 3. The percent increase of each gas over the expected value is given by Eq. 3 below.

$$\text{Percent Increase} = \frac{\text{Gas}_{\text{observed}} - \text{Gas}_{\text{expected}}}{\text{Gas}_{\text{expected}}} \times 100 \quad (3)$$

Independent of the type of polysaccharides co-pyrolyzed, increased gas generation is a strong indicator of enhanced devolatilization and minimized (re)condensation of devolatilized compounds. Therefore,

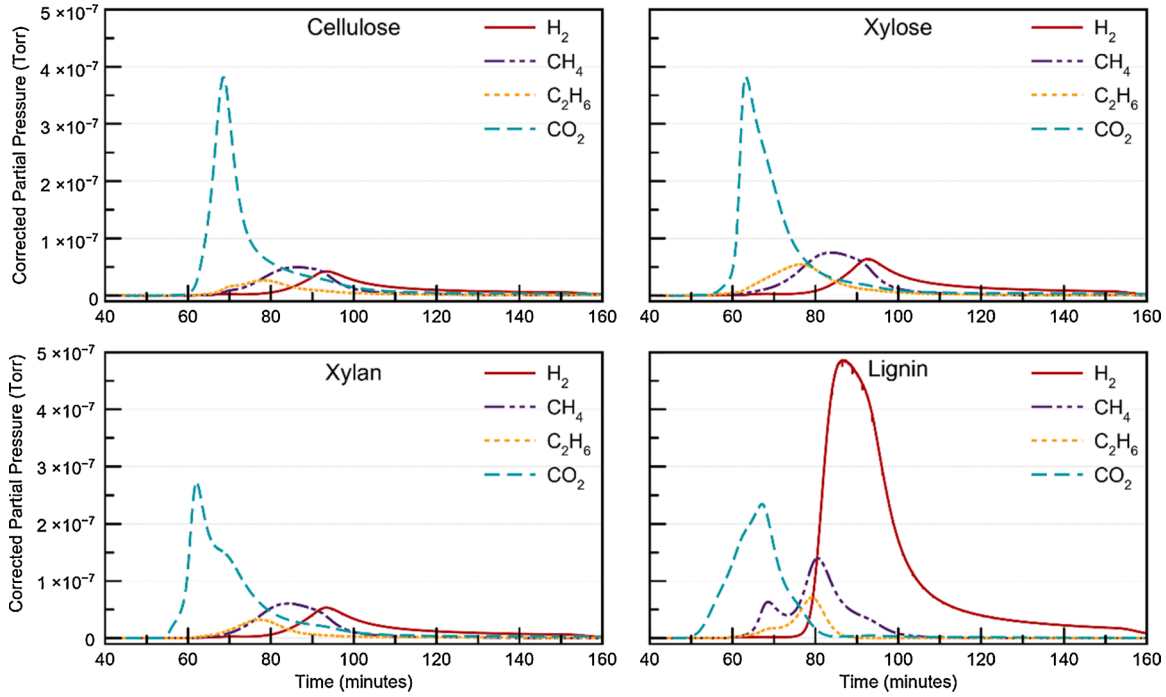

Fig. 2. Pyrolysis gas evolution for individual biomass constituent compounds.

Table 3
Percent difference between observed and expected gas evolution calculated via Eqn. 3, positive values indicate synergistic (non-additive) behavior with enhanced gas evolution.

Pyrolysis Feedstock (Mixtures are equal mass)	Hydrogen (%)	Methane (%)	Ethane (%)	Carbon Dioxide (%)
Cellulose + Lignin	58	24	90	55
Cellulose + Xylan	55	39	38	42
Cellulose + Xylose	26	18	8	16
Lignin + Xylan	71	32	101	80
Lignin + Xylose	68	22	35	66
Xylan + Xylose	15	5	−21	13
Cellulose + Xylan + Lignin	101	40	126	75
Cellulose + Xylose + Lignin	103	38	73	67

pure biomass constituents produce larger amounts of condensed phases (biochar and bio-oil) fractions than mixtures, which favor non-condensable gas formation.

Only ethane production in the xylan + xylose scenario produced less than expected amount (where xylan and xylose mixture remained close to all the predictions). Since these are the monomer and polymer form of the same sugar, this is likely due to the xylan readily depolymerizing into xylose, generating a rather homogeneous mixture without much opportunity for synergism to occur.

The cellulose + xylose mixture generated the second-lowest increase in non-condensable gases over the expected value. Xylose (already in monomer form) and cellulose (which depolymerizes at relatively low temperatures likely again form a somewhat homogenous mixture, whereby their rapidly released gases escape the matrix with little time for heterogeneous reactions.

A subset of the gas evolution can be seen in Fig. 3. The presence of lignin in a mixture drives peak mass loss to lower temperatures and increases the overall hydrogen generation. This suggests that lignin-containing mixtures are desirable for applications where high biochar or high non-condensable gas yields are desirable, such as solids for soil amendments [44] or hydrogen gas for ammonia production [45]. However, the gas evolution in lignin-containing mixtures does not follow the expected additive prediction. Significant increases in both carbon dioxide and hydrogen gas production across all lignin-containing mixtures indicate that the presence of lignin spurs devolatilization and potentially breaks the lignocellulosic components into smaller non-condensable compounds.

3.3. Gas chromatography - mass spectroscopy

The bio-oil results were normalized to the amount of raw biomass loaded in the pyrolysis boats. To enable a comparative analysis between all three outputs (biochar, bio-oil, and pyrolysis gas), decreases or increases in yield are important in determining how the other product yields should respond. All biomasses were analyzed individually – seen in Fig. 4 – and used to develop expected chromatograms based on relative concentrations of the most abundant compounds of the mixtures outlined in Table 1.

Lignin – having the least amount of volatile matter with a complex long-range structure – produced the least amount of bio-oil. The lignin-derived oil contained more phenolic compounds, which agrees with the literature [46]. Given the high content of C6s in lignin's structure, the decomposition favored ethyl group cleavage. Xylose and xylan are known to produce high concentrations of furfural [21,47], which is confirmed by this work. Xylose, xylan, and cellulose individually produced similar amounts of oil in this study as seen in Table 4. Cellulose produces the widest array of compounds and is responsible for most of the higher molecular weight compounds which elute beyond a retention time of 20 min.

Fig. 5 highlights the top ten chromatogram peaks for the cellulose and lignin mixture, and compares them to the expected (additive, non-synergistic) behavior. (Additional chromatograms available in

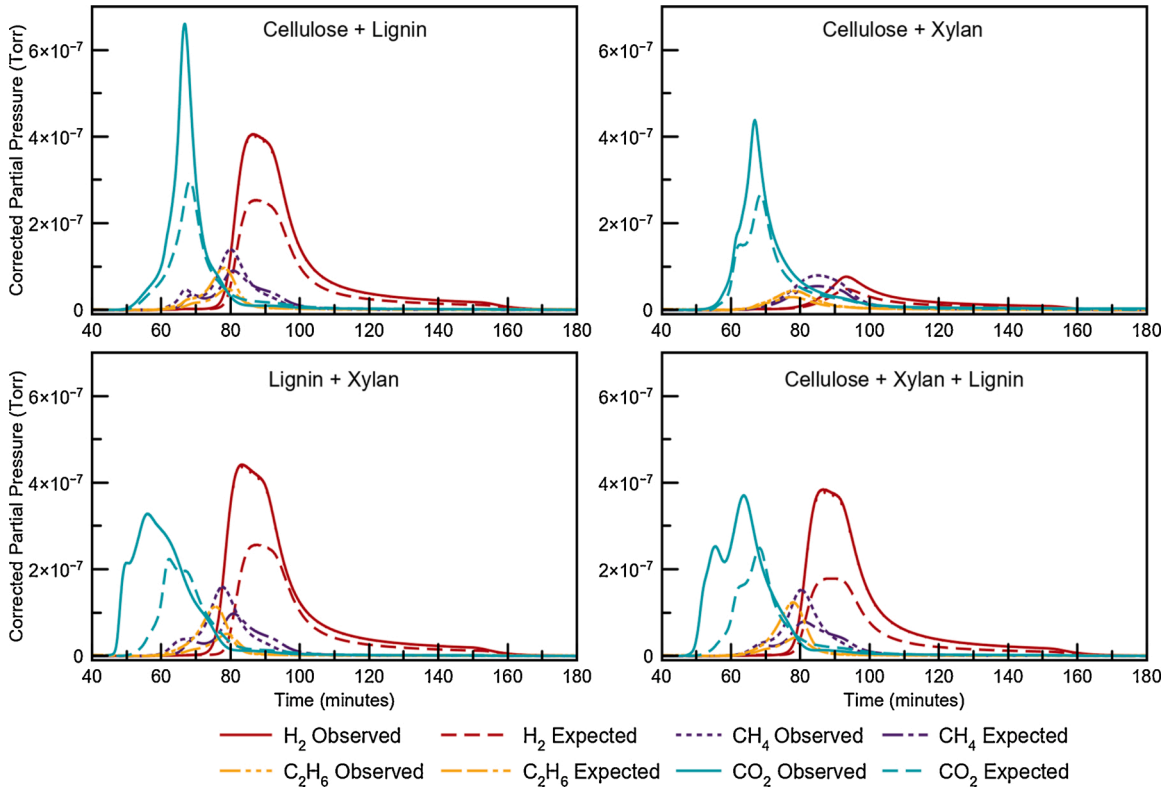

Fig. 3. Pyrolysis gas evolution for select biomass mixtures (additional in SI).

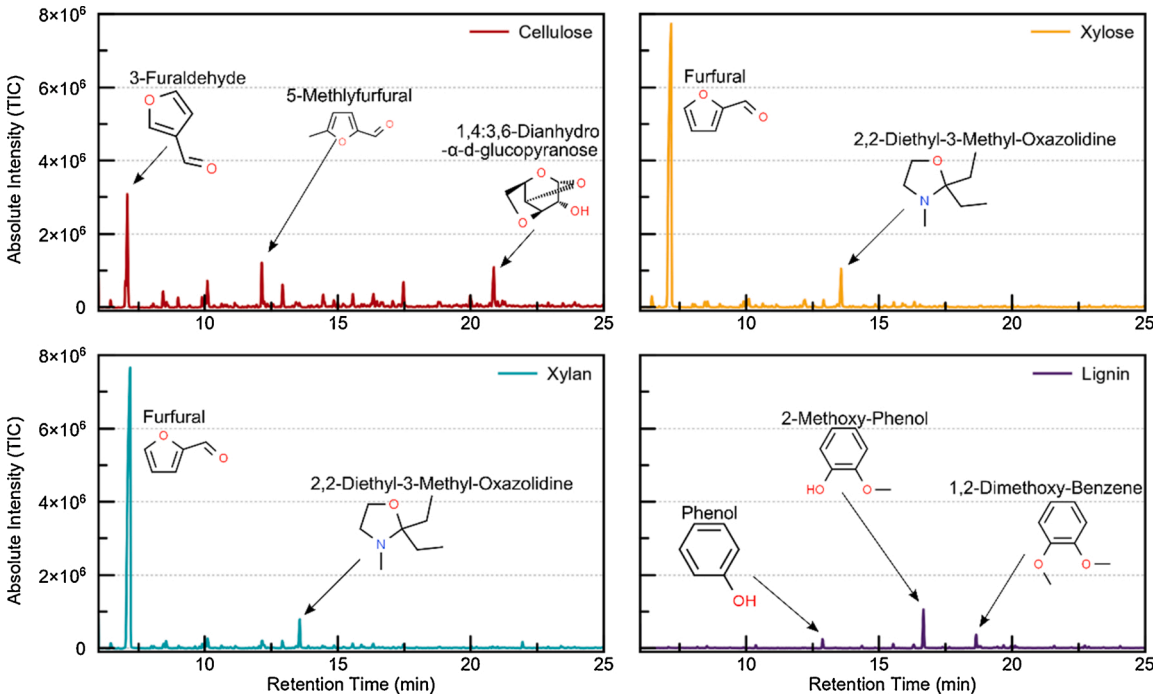

Fig. 4. GC chromatograms of bio-oil for individual biomasses.

Table 4
Bio-oil yield for pure components and mixtures with estimated furan and phenol concentrations.

	Oil Yield (wt %)	Oil Expected (wt %)	Percent Change (%)		Actual (μg/mL)	Expected (μg/mL)	Percent Change (%)
Cellulose	53.1	—	—	Furans	35,504	—	—
				Phenols	26,109	—	—
Xylose	55.7	—	—	Furans	86,321	—	—
				Phenols	2,726	—	—
Xylan	51.8	—	—	Furans	96,919	—	—
				Phenols	3,267	—	—
Lignin	23.3	—	—	Furans	264	—	—
				Phenols	69,997	—	—
Cellulose + Lignin	33.1	37.9	-12.6	Furans	20,791	27,625	**-24.7**
				Phenols	50,068	29,974	**67.0**
Cellulose + Xylose	50.4	54.2	-7.0	Furans	51,890	64,881	**-20.0**
				Phenols	5,630	6,473	**-13.0**
Cellulose + Xylan	52.1	53.5	-2.7	Furans	65,206	102,206	**-36.6**
				Phenols	6,593	6,482	**1.7**
Lignin + Xylose	34.4	39.4	-12.7	Furans	7,323	64,580	**-88.7**
				Phenols	41,578	13,856	**200.1**
Lignin + Xylan	37.2	37.4	-0.5	Furans	4,068	51,517	**-92.1**
				Phenols	28,915	13,508	**114.1**
Xylose + Xylan	53.6	53.6	0	Furans	91,908	85,486	**7.5**
				Phenols	8,078	4,216	**91.6**
Cellulose + Xylose + Lignin	35.6	43.9	-18.9	Furans	13,241	54,273	**-75.6**
				Phenols	31,768	17,191	**84.8**
Cellulose + Xylan + Lignin	38.8	42.5	-8.8	Furans	16,706	62,485	**-73.7**
				Phenols	52,431	17,569	**198.4**

supplemental information.) The dashed lines in Fig. 5 (referred to as zones) group similar compounds based on retention time. Zone one predicted a significant generation of 3-furaldehyde due to the cellulose. However, the mixture formed cyclopentenone in addition to 3-furaldehyde, which had not been present in either the cellulose or lignin cases individually. Additionally, the amount of generated 3-furaldehyde and cyclopentenone combined is only half of the expected 3-furaldehyde amount – the formation of these smaller aromatics was suppressed by the presence of lignin. In contrast, zone 8 generated over 2.5 times the expected 2-methoxy-phenol. The interaction of cellulose and lignin produced more 2-methoxy-phenol than four times as much lignin would have produced on its own. Devolatilizing cellulose may re-condense on

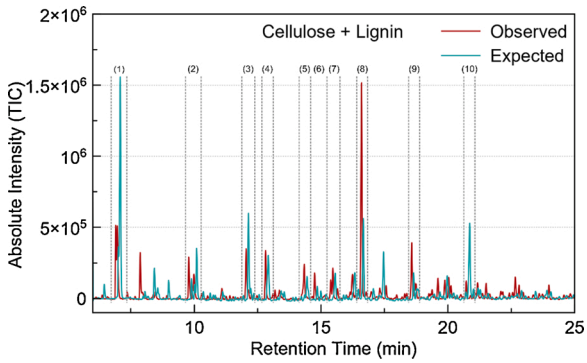

Fig. 5. Cellulose and lignin bio-oil chromatogram.

the lignin surface, forming tar compounds, and preventing the devolatilization of low molecular weight compounds. The increase in phenols potentially stems from cellulose increasing the scission of the oxygen linking individual monolignols, such as β-O-4 which composes more than half of all lignin linkage types [48]. Another significant improvement in the cellulose-lignin mixture was the suppression of the undesired tar compound 1,4:3,6-Dianhydro-α-d-glucopyranose (glucopyranose) in zone 10, which formed only 1/6 of the expected amount.

The most prevalent compounds were identified and semi-quantitatively analyzed. A 50 % reduction in peak area translates to 50 % lower yield. In all cases except xylose + xylan, total pyrolysis bio-oil yield was less than expected. This, in part, corresponds to the non-condensable gas increase seen for the mixtures, in which xylose + xylan was the only mixture to not see significant increases in overall gas production. The non-synergistic behavior of xylose + xylan is likely due to the mixture being the most homogenous.

Bio-oil compounds were split into two major category classes: furans and phenols. Lignin, being a strong phenol generator, led to greater-than-expected concentrations of phenols largely at the expense of furans (highlighted in red in Table 4). In all cases except xylose + xylan, furan production was depressed, potentially contributing to the overall decrease in bio-oil formation and increase in non-condensable gases. While the mechanism of increased phenol generation is not well understood, the mixture of compound classes does not appear to be promoting devolatilization at the expense of biochar formation. Table 5 highlights the biochar formation during each trial. Species containing cellulose resulted in an increase in biochar over their non-cellulose containing counterparts.

Overall, lignin-containing mixtures produce more non-condensable gases, more biochar, and less bio-oil than mixtures that don't contain lignin, suggesting that the increased phenols are not derived at the expense of the solid or gas phases but are a result of the depressed oil generated. The degree of changes to the biochar, bio-oil, and non-condensable gas yield and composition indicates synergistic (non-adaptive) behavior of the polysaccharides. Strong synergistic behavior was seen across polysaccharide classes, where the least synergistic behavior was observed in the mixture containing two forms of the same hemicellulose (xylose and xylan). Mixtures across classes (e.g. hemicellulose and lignin, or cellulose and lignin) promoted non-condensable gas generation and suppressed bio-oil formation. Selecting feedstocks high in lignin may help produce low quantities phenol-rich bio-oil. While lignin produces high amounts of biochar, mixtures containing cellulose produce more biochar than expected. Feedstocks selected to produce biochar soil for amendments benefit from a well-diversified feedstock, balancing the increased yield from lignin and increased synergy from cellulose.

Table 5
Weight percent of biochar formed versus predicted from pyrolysis of pure polysaccharides and mixtures.

	Biochar Produced (wt %)	Biochar Expected (wt %)	Percent Change (%)
Cellulose	17.8	—	—
Xylose	18.9	—	—
Xylan	17.9	—	—
Lignin	58.4	—	—
Cellulose + Lignin	38.5	37.9	1.5
Cellulose + Xylose	19.8	18.3	8.1
Cellulose + Xylan	20.2	18.2	10.6
Lignin + Xylose	34.3	38.5	−11.0
Lignin + Xylan	33.8	38.1	−11.1
Xylose + Xylan	15.5	18.3	−15.8
Cellulose + Xylose + Lignin	33.3	31.6	5.2
Cellulose + Xylan + Lignin	34.5	31.3	10.3

4. Conclusions

The selection of biomass feedstocks for pyrolytic conversion to bio-based fuels plays an important role in the composition of non-condensable gases, biochar, and bio-oil produced. To aid in the selection of biomasses to better target desired products, an understanding of the synergistic interactions between constituent polysaccharides is required. Biomass polysaccharides undergoing pyrolysis exhibit synergistic behavior, promoting non-condensable gas evolution and suppressing the formation of furans. Lignin-containing mixtures promote hydrogen gas formation, by potentially favoring C—C and C—O bonds to generate increased biochar over bio-oil yield. Additionally, lignin-containing mixtures promote phenols in bio-oil, likely formed through greater oxygen scission of the monolignol linkages. Cellulose-containing mixtures result in increased biochar yield possibly through condensation of tar compounds on the biochar surface. These findings suggest that cellulose, xylan, xylose, and lignin synergistically interact with each other, generating different concentrations of compounds than would be expected by a summation of their individual parts. Better understanding of the interactions behind the synergistic behavior helps guide targeted feedstock and mixture ratios to improve the quality of the bio-oil: improving stability, energy density, and viscosity.

CRediT authorship contribution statement

Andrew H. Hubble: Conceptualization, Methodology, Investigation, Writing - original draft. **Jillian L. Goldfarb:** Conceptualization, Methodology, Writing – Original Review & Editing, Resources, Funding acquisition, Supervision.

Declaration of Competing Interest

The authors report no declarations of interest.

Acknowledgements

This work was supported by the National Science Foundation under grant number 1933071 and by the Eppley Foundation for Research.

Appendix A. Supplementary data

Supplementary material related to this article can be found, in the online version, at doi:https://doi.org/10.1016/j.jaap.2021.105100.

References

[1] R. Prinn, M. John, M. Sarofim, C. Wang, B. Felzer, Effects of air pollution control on climate: results from an integrated global system model, Hum.-Induced Clim. Change. Interdiscip. Assess. (2007) 93–102, 9780521866.

[2] A.V. Bridgwater, Review of fast pyrolysis of biomass and product upgrading, Biomass Bioenergy 38 (2012) 68–94.
[3] A.V. Bridgwater, G.V.C. Peacocke, Fast pyrolysis processes for biomass, Renew. Sustain. Energy Rev. 4 (2000) 1–73.
[4] S. Czernik, A.V. Bridgwater, Overview of applications of biomass fast pyrolysis oil, Energy Fuels 18 (2004) 590–598.
[5] K. Jedvert, T. Heinze, Cellulose modification and shaping - a review, J. Polym. Eng. 37 (2017) 845–860.
[6] X. Zhou, W. Li, R. Mabon, L.J. Broadbelt, A critical review on hemicellulose pyrolysis, Energy Technol. 5 (2017) 52–79.
[7] L. Yang, K. Seshan, Y. Li, A review on thermal chemical reactions of lignin model compounds, Catal. Today 298 (2017) 276–297.
[8] V. Pasangulapati, et al., Effects of cellulose, hemicellulose and lignin on thermochemical conversion characteristics of the selected biomass, Bioresour. Technol. 114 (2012) 663–669.
[9] A. Demirbaş, Mechanisms of liquefaction and pyrolysis reactions of biomass, Energy Convers. Manage. 41 (2000) 633–646.
[10] M. Balat, Mechanisms of thermochemical biomass conversion processes. Part 1: reactions of pyrolysis, Energy Sources Part A Recover. Util. Environ. Eff. 30 (2008) 620–635.
[11] N.M. Bennett, S.S. Helle, S.J.B. Duff, Extraction and hydrolysis of levoglucosan from pyrolysis oil, Bioresour. Technol. 100 (2009) 6059–6063.
[12] X. Bai, R.C. Brown, Modeling the physiochemistry of levoglucosan during cellulose pyrolysis, J. Anal. Appl. Pyrolysis 105 (2014) 363–368.
[13] C.H. Ashman, L. Gao, J.L. Goldfarb, Silver nitrate in situ upgrades pyrolysis biofuels from Brewer's spent grain via Biotemplating, J. Anal. Appl. Pyrolysis 104729 (2019), https://doi.org/10.1016/j.jaap.2019.104729.
[14] Q. Zhang, J. Chang, T. Wang, Y. Xu, Review of biomass pyrolysis oil properties and upgrading research, Energy Convers. Manage. 48 (2007) 87–92.
[15] X.L. Zhuang, H.X. Zhang, J.Z. Yang, H.Y. Qi, Preparation of levoglucosan by pyrolysis of cellulose and its citric acid fermentation, Bioresour. Technol. 79 (2001) 63–66.
[16] J. Wang, Q. Wei, J. Zheng, M. Zhu, Effect of pyrolysis conditions on levoglucosan yield from cotton straw and optimization of levoglucosan extraction from bio-oil, J. Anal. Appl. Pyrolysis 122 (2016) 294–303.
[17] G.F. David, O.R. Justo, V.H. Perez, M. Garcia-Perez, Thermochemical conversion of sugarcane bagasse by fast pyrolysis: high yield of levoglucosan production, J. Anal. Appl. Pyrolysis 133 (2018) 246–253.
[18] D.O. Usino, Supriyanto, P. Ylitervo, A. Pettersson, T. Richards, Influence of temperature and time on initial pyrolysis of cellulose and xylan, J. Anal. Appl. Pyrolysis 104782 (2020), https://doi.org/10.1016/j.jaap.2020.104782.
[19] F.Z. Belmokaddem, C. Pinel, P. Huber, M. Petit-Conil, D. Da Silva Perez, Green synthesis of xylan hemicellulose esters, Carbohydr. Res. 346 (2011) 2896–2904.
[20] S.K. Dutta, S. Chakraborty, Kinetic analysis of two-phase enzymatic hydrolysis of hemicellulose of xylan type, Bioresour. Technol. 198 (2015) 642–650.
[21] W. Wang, J. Ren, H. Li, A. Deng, R. Sun, Direct transformation of xylan-type hemicelluloses to furfural via SnCl4 catalysts in aqueous and biphasic systems, Bioresour. Technol. 183 (2015) 188–194.
[22] N. Syaftika, Y. Matsumura, Comparative study of hydrothermal pretreatment for rice straw and its corresponding mixture of cellulose, xylan, and lignin, Bioresour. Technol. 255 (2018) 1–6.
[23] J.J. Bozell, G.R. Petersen, Technology development for the production of biobased products from biorefinery carbohydrates—the US Department of Energy's "top 10" revisited, Green Chem. 12 (2010) 539–555.
[24] O. Beaumont, Flash pyrolysis products from beech wood, Wood Fiber Sci. 17 (1985) 228–239.
[25] T.K. Ormond, et al., Thermal decompositions of the lignin model compounds: salicylaldehyde and catechol, J. Phys. Chem. A 122 (2018) 5911–5924.
[26] Y.C. Chang, D.B. Choi, K. Takamizawa, S. Kikuchi, Isolation of Bacillus sp. strains capable of decomposing alkali lignin and their application in combination with lactic acid bacteria for enhancing cellulase performance, Bioresour. Technol. 152 (2014) 429–436.
[27] M. Asmadi, H. Kawamoto, S. Saka, Thermal reactivities of catechols/pyrogallols and cresols/xylenols as lignin pyrolysis intermediates, J. Anal. Appl. Pyrolysis 92 (2011) 76–87.
[28] H. Kawamoto, Lignin pyrolysis reactions, J. Wood Sci. 63 (2017) 117–132.
[29] M.M. Jaffar, M.A. Nahil, P.T. Williams, Pyrolysis-catalytic hydrogenation of cellulose-hemicellulose-lignin and biomass agricultural wastes for synthetic natural gas production, J. Anal. Appl. Pyrolysis 145 (2020), 104753.
[30] H. Yang, et al., Vapor–solid interaction among cellulose, hemicellulose and lignin, Fuel 263 (2020), 116681.
[31] J. Xue, S. Ceylan, J.L. Goldfarb, Synergism among biomass building blocks? Evolved gas and kinetics analysis of starch and cellulose co-pyrolysis, Thermochim. Acta 618 (2015) 36–47.
[32] Q. Liu, Z. Zhong, S. Wang, Z. Luo, Interactions of biomass components during pyrolysis: a TG-FTIR study, J. Anal. Appl. Pyrolysis 90 (2011) 213–218.
[33] W.H. Chen, P.C. Kuo, Torrefaction and co-torrefaction characterization of hemicellulose, cellulose and lignin as well as torrefaction of some basic constituents in biomass, Energy 36 (2011) 803–811.
[34] S. Vyazovkin, et al., ICTAC Kinetics Committee recommendations for analysis of multi-step kinetics, Thermochim. Acta 689 (2020), 178597.
[35] M. Wang, Z. Li, W. Huang, J. Yang, H. Xue, Coal pyrolysis characteristics by TG-MS and its late gas generation potential, Fuel 156 (2015) 243–253.
[36] F. Shafizadeh, A.G.W. Bradbury, Thermal degradation of cellulose in air and nitrogen at low temperatures, J. Appl. Polym. Sci. 23 (1979) 1431–1442.
[37] M. Lewin, A. Basch, Structure, pyrolysis, and flammability of cellulose. Flame - Retardent Polymeric Materials, Springer, 1978, https://doi.org/10.1007/978-1-4684-6973-8_1.
[38] R. Volpe, A.A. Zabaniotou, V. Skoulou, Synergistic effects between lignin and cellulose during pyrolysis of agricultural waste, Energy Fuels 32 (2018) 8420–8430.
[39] J. Zhang, et al., Cellulose-hemicellulose and cellulose-lignin interactions during fast pyrolysis, ACS Sustain. Chem. Eng. 3 (2015) 293–301.
[40] J. Huang, C. He, L. Wu, H. Tong, Thermal degradation reaction mechanism of xylose: a DFT study, Chem. Phys. Lett. 658 (2016) 114–124.
[41] M. Jablonsky, M. Botkova, J. Adamovska, Prediction of methoxyl groups content in lignin based on ultimate analysis, Cellulose Chem. Technol. 49 (2015).
[42] O. Faix, E. Jakab, F. Till, T. Székely, Study on low mass thermal degradation products of milled wood lignins by thermogravimetry-mass-spectrometry, Wood Sci. Technol. 22 (1988) 323–334.
[43] Q. Lu, et al., A novel interaction mechanism in lignin pyrolysis: phenolics-assisted hydrogen transfer for the decomposition of the β-O-4 linkage, Combust. Flame 225 (2021) 395–405.
[44] J. Lehmann, S. Joseph, Biochar for environmental management: science and technology. Biochar for Environmental Management: Science and Technology, Earthscan, 2009.
[45] Geoffrey Skinner, P. F. & Kowal, W. M. United States Patent (19) Skinner et al. 54 Synthesis gas for ammonia. (1981).
[46] P. Zong, et al., Pyrolysis behavior and product distributions of biomass six group components: starch, cellulose, hemicellulose, lignin, protein and oil, Energy Convers. Manage. 216 (2020), 112777.
[47] Z. Gao, N. Li, Y. Wang, W. Niu, W. Yi, Pyrolysis behavior of xylan-based hemicellulose in a fixed bed reactor, J. Anal. Appl. Pyrolysis 146 (2020), 104772.
[48] J. Zakzeski, P.C.A. Bruijnincx, A.L. Jongerius, B.M. Weckhuysen, The catalytic valorization of lignin for the production of renewable chemicals, Chem. Rev. 110 (2010) 3552–3599.